Thermal Unfolding of Apo and Holo *Desulfovibrio desulfuricans* Flavodoxin: Cofactor Stabilizes Folded and Intermediate States†

B. K. Muralidhara‡ and Pernilla Wittung-Stafshede*,‡,§

Department of Biochemistry and Cell Biology and Department of Chemistry, Rice University, Houston, Texas 77251

Received May 24, 2004; Revised Manuscript Received July 7, 2004

ABSTRACT: We here compare thermal unfolding of the apo and holo forms of *Desulfovibrio desulfuricans* flavodoxin, which noncovalently binds a flavin mononucleotide (FMN) cofactor. In the case of the apo form, fluorescence and far-UV circular dichroism (CD) detected transitions are reversible but do not overlap (T_m of 50 and 60 °C, respectively, pH 7). The thermal transitions for the holo form follow the same pattern but occur at higher temperatures (T_m of 60 and 67 °C for fluorescence and CD transitions, respectively, pH 7). The holoprotein transitions are also reversible and exhibit no protein concentration dependence (above 10 μM), indicating that the FMN remains bound to the polypeptide throughout. Global analysis shows that the thermal reactions for both apo and holo forms proceed via an equilibrium intermediate that has ∼90% nativelike secondary structure and significant enthalpic stabilization relative to the unfolded states. Incubation of unfolded holoflavodoxin at high temperatures results in FMN dissociation. Rebinding of FMN at these conditions is nominal, and therefore, cooling of holoprotein heated to 95 °C follows the refolding pathway of the apo form. However, FMN readily rebinds to the apoprotein at lower temperatures. We conclude that (1) a three-state thermal unfolding behavior appears to be conserved among long- and short-chain, as well as apo and holo forms of, flavodoxins and (2) flavodoxin's thermal stability (in both native and intermediate states) is augmented by the presence of the FMN cofactor.

Many proteins fold spontaneously in vitro, but the mechanisms of such processes are not fully understood. In addition to the native and unfolded states, proteins can adopt conformations, either transiently or at equilibrium, which display mixed properties of the native and denatured states. It is often found that small proteins fold by two-state equilibrium and kinetic mechanisms whereas proteins longer than 100 residues often go through intermediate structures in their equilibrium and/or kinetic folding reactions (*1*). Such intermediates may be on-pathway, facilitating the reaction, or off-pathway, acting as traps that may lead to aggregation (*2*, *3*). Equilibrium intermediates can be detected in vitro as a deviation from two-state behavior, i.e., noncoincident protein unfolding curves obtained with different experimental techniques (*4*), although their structures and energetic properties are more difficult to probe. Since many proteins in the cells coordinate cofactors (such as metal ions or organic moieties) to attain specific functions, the role of cofactors in folding of such proteins must be considered (*5*). As demonstrated in vitro, many cofactor-binding proteins (for example, cytochrome b_{562}, myoglobin, azurin, and the Cu_A domain) are capable of retaining specific interactions with the cofactor after polypeptide unfolding, even without covalent bonds linking the protein and cofactor (*6*−*9*). This implies that cofactors can interact with their corresponding proteins before polypeptide folding and, therefore, the cofactors may impact the folding reaction and affect intermediate structures (*10*, *11*).

In contrast to most protein folds, the flavodoxin-like fold is shared by nine protein superfamilies (*12*). These superfamilies exhibit little or no sequence similarity and comprise a broad range of unrelated proteins with different functions, such as catalases, chemotactic proteins, lipases, esterases, and flavodoxins. Still, they are all characterized by a fold containing a five-stranded parallel β-sheet surrounded by α-helices at either side of the sheet (*12*) (Figure 1A). The small size and well-established physical and structural properties make flavodoxins good model systems for folding studies aiming toward defining fundamental rules for folding of proteins with the flavodoxin-like fold. In addition, flavodoxins are useful systems for characterization of the interplay between polypeptide folding and cofactor interactions. There are two types of flavodoxins: long- and short-chain variants (*12*). Long-chain flavodoxins (such as *Azotobacter vinelandii* and *Anabaena* PCC 7119) only differ from short-chain versions (such as *Desulfovibrio desulfuricans*, *Desulfovibrio vulgaris*, and *Clostridium beijerinckii*) in that they have a 20−25 residue loop that interrupts β-strand 5 (Figure 1B). All flavodoxins contain a single,

† The National Institutes of Health are acknowledged for financial support (GM59663).

* To whom correspondence should be addressed at the Department of Biochemistry and Cell Biology. Phone: 713-348-4076. Fax: 713-348-5154. E-mail: pernilla@rice.edu.

‡ Department of Biochemistry and Cell Biology, Rice University.

§ Department of Chemistry, Rice University.

10.1021/bi048944e CCC: $27.50 © 2004 American Chemical Society
Published on Web 09/11/2004

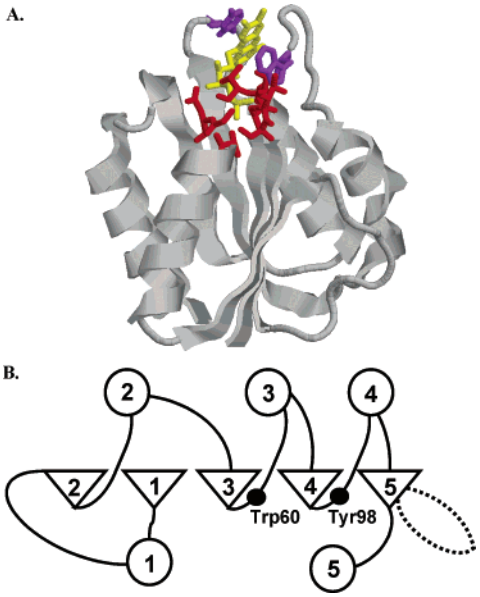

FIGURE 1: (A) Representation of the three-dimensional structure of flavodoxin. The cartoon (atomic coordinates from PDB entry 2fx2; *D. vulgaris* flavodoxin) displays the secondary structure elements (α-helices, β-strands, and loops) and the side chains of Trp60 and Tyr98 (purple) and residues 10−15 as well as residues 58−59 (red). The FMN cofactor is shown in yellow. The isoalloxazine ring of the FMN stack with Trp60 and Tyr98 and the phosphate tail makes hydrogen bond contacts with Ser10, Thr11, Thr12, Gly13, Asn14, and Thr15 (constituting the conserved phosphate-binding motif S/T-X-T-G-X-T) as well as Ser58 and Thr59. (B) Schematic drawing of the topology of flavodoxins. The long-chain variants only differ from the short-chain variants in that there is an extra (>20 residues) loop interrupting β-strand 5 (dotted loop). The helices (shown as circles) and strands (shown as triangles) are labeled from the N- to C-terminus. The connecting loops are represented as lines. We note that helix 2 is extremely short in *D. vulgaris* flavodoxin (panel A). The positions of Trp60 and Tyr98, stacking with the FMN aromatic rings, are indicated. Residues 10−15, interacting with the phosphate of FMN, are situated between strand 1 and helix 1.

noncovalently bound flavin mononucleotide (FMN)[1] cofactor and function as low-potential one-electron carriers. Cofactor binding occurs primarily through a combination of hydrogen bonds and aromatic interactions with the apoprotein (*13*, *14*). The FMN interacts with three loops of the protein: two aromatic residues (Tyr60 and Trp98 in *D. desulfuricans* flavodoxin, Figure 1A), located on opposite loops (residues 58−66 and 95−102 in *D. desulfuricans*), flank either side of the FMN isoalloxazine ring, allowing for π-orbital overlap. The 5′-phosphate moiety of FMN is bound in an atypical phosphate-binding site, anchored by several hydrogen bonds in a loop near the N-terminus, but with no ion-pairing interactions (*13*, *15*). The phosphate-binding motif, Ser/Thr-X-Thr-Gly-X-Thr, is highly conserved in all flavodoxins and corresponds to Ser10, Thr11, Thr12, Gly13, Asn14, and Thr15 in *D. desulfuricans* (Figure 1A). Upon FMN removal in *A. vinelandii* and *Anabaena* PCC 7119 flavodoxins, the apoprotein adopts a structure that is identical to that of the holo form, except for more dynamics observed by NMR in the FMN-binding loop regions (*15*, *16*).

[1] Abbreviations: CD, circular dichroism; FMN, flavin mononucleotide; ITC, isothermal titration calorimetry; K_D, dissociation constant; T_m, temperature at midpoint of thermal transition; GuHCl, guanidine hydrochloride; N, native state; I, intermediate state; U, unfolded state.

Thermal and chemical unfolding studies of flavodoxins in vitro have focused on the apo forms of the long-chain flavodoxins from *A. vinelandii* and *Anabaena* PCC 7119. It was shown for both of these apoproteins that thermal unfolding involves a relatively stable intermediate described as a molten globule (*17*−*19*). However, chemically induced equilibrium unfolding of apoflavodoxin from *Anabaena* PCC 7119 was found to be a simple two-state process (*20*) whereas chemically induced equilibrium unfolding of apoflavodoxin from *A. vinelandii* was similar to the thermal unfolding process, involving a stable intermediate (*17*, *18*). We have earlier reported GuHCl-induced equilibrium unfolding studies of the short-chain flavodoxin (148 residues) from *D. desulfuricans* ATCC strain 29577 in both apo and holo forms (pH 7, 20 °C). We found that chemically induced unfolding of this protein, regardless of the presence or absence of the cofactor, is a two-state reaction; in the case of the holo form, the FMN remains associated with the polypeptide upon unfolding (*21*, *22*). The cofactor stabilizes the flavodoxin-like fold by roughly 6 kJ/mol toward chemical denaturation (pH 7, 20 °C). There has been one report on urea-induced unfolding of the short-chain *D. vulgaris* flavodoxin (*23*); however, there have been no thermal unfolding studies of any short-chain flavodoxin nor has there been any such studies of a holoflavodoxin.

Here, we report on the thermal unfolding reaction for the short-chain *D. desulfuricans* flavodoxin in both apo and holo forms. The unfolding behavior (pH 7) for both apo and holo forms agrees with those proposed for long-chain apoflavodoxins: it includes the presence of an equilibrium intermediate populated up to 70% at intermediate temperatures. Global analysis reveals that the intermediate, for both apo and holo forms, has nativelike secondary structure and retains ∼60% of the interactions that contribute to the enthalpic stabilization of the native state. The presence of the FMN stabilizes the native, as well as the intermediate, states toward thermal perturbation. FMN does not dissociate from the unfolded holoprotein until very high temperatures are reached. Rebinding of FMN at these conditions is negligible, and therefore, cooling of holoflavodoxin starting at 95 °C (i.e., unfolded polypeptide and free FMN) follows the pathway of the apo form: the polypeptide refolds to the nativelike apo intermediate before FMN rebinds.

MATERIALS AND METHODS

Protein Preparation. Flavodoxin from *D. desulfuricans* (ATCC strain 29577) was expressed in *Escherichia coli* (*24*) and purified as described previously (*25*, *26*) with some modifications. Apo- and holoflavodoxin were eluted separately on a Q-Sepharose column and further purified individually by gel permeation on a Superdex-75 using FPLC (Amersham-Pharmacia) (*27*). Purified apoflavodoxin (>99% pure) and HPLC-purified FMN (Sigma Chemicals) were used in all binding studies. FMN was oxidized in all experiments and its concentration determined using a molar extinction coefficient of $\epsilon_{445\ nm} = 12500\ M^{-1}\ cm^{-1}$.

Thermal Unfolding−*Refolding Reactions*. Apo- and holoflavodoxin unfolding and refolding experiments were carried out by monitoring CD at 222 nm on a circular dichroism spectrometer (Aviv 62A DS, single cell Peltier) and emission on a spectrofluorometer [Cary Eclipse (Varian), multicell

Peltier] as a function of temperature. For apoflavodoxin, fluorescence at 350 nm (excitation 285 nm) was monitored; for holoflavodoxin, emission was monitored both at 350 nm (aromatics, excitation 285 nm) and at 525 nm (FMN, excitation 445 nm). Protein concentrations were varied from 1 to 50 μM in the experiments, as described in the legends. Both unfolding (from 25 to 95 °C) and refolding (from 95 to 25 °C) data points were collected every degree (°C) with a 5 °C/min scan rate and a 12 s equilibration time at each temperature before data collection (each data point averaged for 5 s). The temperature was held for 2 min at 95 °C before the start of the cooling process. In some holoprotein unfolding−refolding experiments, heating was only continued up to 80 °C before cooling was started. Scan rates (in both far-UV CD and fluorescence experiments) were varied between 0.5 and 20 °C/min to check for any scan rate dependences in the unfolding−refolding processes.

Thermal Data Analysis. Each data set was fit to a two-state transition to obtain the midpoint temperature (T_m) for each particular transition. We first assumed a three-state equilibrium unfolding pathway involving folded (F), intermediate (I), and unfolded (U) conformations:

$$F \leftrightarrow I \leftrightarrow U$$

in which the intermediate and unfolded forms have identical fluorescence (Fl) signals ($Fl_I = Fl_U$) and the folded and intermediate forms have identical CD signals ($CD_I = CD_F$). These constraints allowed us to use the fluorescence transitions to estimate the fraction of native protein (f_F) and the CD transitions to estimate the fraction unfolded (f_U) at each temperature. Then using the relation $1 = f_F + f_U + f_I$, we could derive the fraction of intermediate at each temperature (f_I). This simplified analysis has been used previously to characterize apoflavodoxin unfolding (*18*, *22*).

We also performed global analysis of the spectroscopic data to a three-state equilibrium unfolding pathway, again involving F, I, and U conformations. We followed the approach described by Luo et al. (*28*) that has subsequently been used to characterize thermal unfolding of *Anabaena* apoflavodoxin (*19*). Global fitting of the fluorescence and far-UV CD-detected unfolding curves for *D. desulfuricans* flavodoxin at various conditions (apo or holo form; different protein concentrations) was performed with the program MATLAB (version 6.5; MathWorks Inc.). The optical data were converted to the apparent fraction of unfolded protein (*28*), f_{app}, using

$$f_{app} = (Y - Y_N)/(Y_U - Y_N)$$

where Y is the observed signal and Y_U and Y_N are the optical signals for unfolded and folded proteins, respectively. Both Y_N and Y_U were observed to depend linearly on the temperature, and the linear dependence was assumed to hold in the transition region. f_{app} can be rewritten in terms of the fractional populations of the intermediate and unfolded species (f_I and f_U) as

$$f_{app} = f_U + Zf_I$$

where $Z = (Y_I - Y_N)/(Y_U - Y_N)$. The Z parameter is the measure of the degree to which the intermediate state spectroscopically resembles the unfolded state. Using the relationship between fractional populations and equilibrium constants, and the balance of fractions ($1 = f_F + f_U + f_I$), f_{app} can be calculated as (*28*)

$$f_{app} = [Z + \exp(-\Delta G_{IU}(T)/RT)]/ [1 + \exp(\Delta G_{NI}(T)/RT) + \exp(-\Delta G_{IU}(T)/RT)]$$

where $\Delta G_{NI}(T)$ and $\Delta G_{IU}(T)$ are defined as

$$\Delta G_{NI}(T) = \Delta H_{NI}(T_{mNI})[1 - T/T_{mNI}] - \Delta C_{pNI}[(T_{mNI} - T) + T \ln(T/T_{mNI})]$$

$$\Delta G_{IU}(T) = \Delta H_{IU}(T_{mIU})[1 - T/T_{mIU}] - \Delta C_{pIU}[(T_{mIU} - T) + T \ln(T/T_{mIU})]$$

In each fitting, all thermodynamic parameters were globally constrained, while the optical properties of the intermediate (the Z values) were allowed to vary between CD and fluorescence detection techniques. [We note that the simple three-state analysis, in which fluorescence reports on the disappearance of folded species and CD reports on the appearance of unfolded species, corresponds to $Z = 1$ for fluorescence and $Z = 0$ for CD in the global analysis.] The ΔC_p values obtained are not reported since they are usually unreliable for this type of data fitting (*29*, *30*).

Cofactor Binding as a Function of Temperature. Thermodynamic binding measurements were made using an isothermal titration calorimeter (VP-ITC, MicroCal) at 20, 40, 50, 60, 65, and 70 °C. Protein and FMN samples were filtered through 0.22 μm sterile filters (Millipore) and degassed (ThermoVac, MicroCal) before being loaded into the ITC cell and syringe. All samples were preequilibrated at the experimental temperature for 1 h in the calorimeter before titrations were started. At least two to three buffer-to-buffer titrations were run to establish accurate baselines. Before FMN−protein binding experiments, reference titrations injecting FMN to buffer were carried out (and subsequently subtracted from the FMN−protein titrations). A typical injection schedule included the addition of 10 μL samples of 1.0 mM FMN to 50 μM apoflavodoxin with 25−28 injections spaced between 3 min intervals. Extreme care was taken to avoid sample evaporation at high experimental temperatures. For each condition studied, at least two independent titrations were performed. The resulting binding isotherms at 20, 40, and 50 °C were fit to a one-set binding-site model by Marquardt nonlinear least-squares analysis (Origin 5.0). Analyses of the binding isotherms at higher temperatures with different binding models yielded unreliable parameters due to parallel binding−folding events and, hence, are not reported.

RESULTS

Thermal Unfolding and Refolding of Apoflavodoxin. Thermal unfolding of *D. desulfuricans* apoflavodoxin was monitored by fluorescence and far-UV circular dichroism (CD) spectral changes, which report on the environment of the tryptophan (Trp60) and secondary structure, respectively. Representative spectra are shown in Figure 2 for the folded (20 °C) and unfolded (90 °C) forms of apoflavodoxin. The emission is quenched, and its maximum shifted by ~10 nm

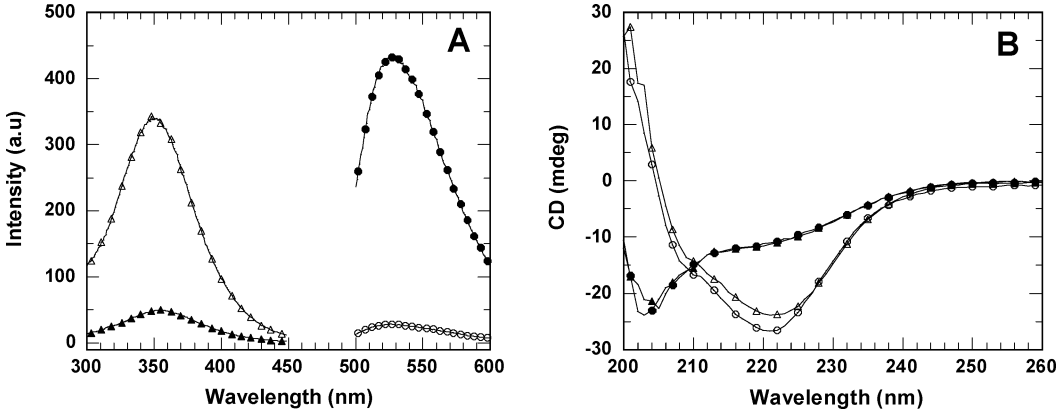

FIGURE 2: Typical spectroscopic changes upon thermal perturbation. Fluorescence (A) and circular dichroism (B) spectra of apoflavodoxin (triangles) and holoflavodoxin (circles) at 20 °C (open symbols) and 90 °C (filled symbols) in 40 mM phosphate, pH 7 (10 μM protein in each case). Fluorescence excitation was at 285 nm (protein aromatics) and 445 nm (FMN) for apo- and holoflavodoxin, respectively.

to higher wavelengths, upon unfolding at high temperatures (Figure 2A). The far-UV CD signal changes from one characteristic of a folded protein, with mixed α/β secondary structure, to one resembling a random coil, when apoflavodoxin unfolds (Figure 2B).

Typical unfolding profiles for apoflavodoxin as monitored by fluorescence and CD are shown in Figure 3A. The two unfolding curves monitored by the different methods are clearly noncoincidental: the thermal midpoint of transition (T_m) is 50 and 60 °C for fluorescence and CD detection, respectively. This shows that the process is not two state but instead involves an intermediate structure. A three-state equilibrium unfolding behavior is similar to earlier observations on long-chain apoflavodoxins (*18*, *19*). Thermal unfolding of *D. desulfuricans* apoprotein is fully reversible, and refolding profiles by both detection methods match the corresponding unfolding profiles giving T_m values of 50 and 60 °C. In Figure 3B we show the observed T_m values for unfolding (heating) and refolding (cooling) of apoflavodoxin when monitored by CD and fluorescence as a function of protein concentration (1−50 μM). It is clear that the fluorescence-detected T_m (50 ± 2 °C) and the CD-detected T_m (60 ± 2 °C) exhibit no protein concentration dependence and are identical within errors regardless of whether unfolding or refolding is tested. There was no scan rate dependence (0.5−20 °C/min tested) in any of the transitions (data not shown), supporting that the transitions are truly equilibrium reactions.

To analyze the thermal data, we first assumed a three-state equilibrium unfolding pathway involving folded (F), intermediate (I), and unfolded (U) species:

$$F \leftrightarrow I \leftrightarrow U$$

in which the intermediate and unfolded forms have identical fluorescence (Fl) signals ($Fl_I = Fl_U$) and the folded and intermediate forms have identical CD signals ($CD_I = CD_F$). Then, the fluorescence transition reports on the disappearance of the folded state and the CD transition reports on the appearance of the unfolded state, and the fraction of intermediate at each temperature is calculated as $f_I = 1 - f_F - f_U$. In Figure 3C, we show the resulting relation between the three species as a function of temperature when making these assumptions.

Thermal Unfolding of Holoflavodoxin. Thermal unfolding of *D. desulfuricans* holoflavodoxin was probed at protein concentrations above the K_D for FMN binding to apoflavodoxin at 20 °C (K_D = 0.1 μM, 40 mM phosphate, pH 7, 20 °C) (*27*). Representative spectra are shown in Figure 2 for folded (20 °C) and unfolded (90 °C) forms of holoflavodoxin. In folded holoflavodoxin, the FMN fluorescence is highly quenched due to aromatic stacking with Trp60 and Tyr98. The FMN emission increases dramatically upon unfolding at higher temperatures, as a result of either destacking from the aromatic residues or complete dissociation from the polypeptide (Figure 2A). Like the apoprotein, the far-UV CD signal of holoflavodoxin changes from one characteristic of a folded protein, with mixed α/β content, to one resembling a random coil, when the protein unfolds (Figure 2B). The negative CD signal of folded holoflavodoxin is slightly larger than that of apoflavodoxin, possibly due to FMN contributions when in the chiral folded protein.

In Figure 4A we show typical unfolding curves for holoflavodoxin (10 μM and higher concentrations) as monitored by fluorescence at 350 nm (excitation 285 nm, aromatics) and 525 nm (excitation 445 nm, FMN) and by far-UV CD at 220 nm. Both fluorescence transitions overlap, exhibiting a T_m of 60 °C. The unfolding curve obtained by far-UV CD is shifted to higher temperatures and has a midpoint of ~67 °C. Albeit the T_m values are shifted to higher temperatures, the thermal unfolding behavior for holoflavodoxin, like the apo form, appears to involve an intermediate species. In Figure 4B, we show the T_m values derived from the fluorescence and CD transitions obtained upon heating as a function of holoprotein concentration. There was no scan rate dependence (0.5−20 °C/min tested) in any of these transitions (data not shown), implying that all transitions are probed at equilibrium. The T_m values of the fluorescence and CD transitions detected upon heating did not exhibit any protein concentration dependence above 10 μM holoprotein. At low protein concentrations (1−2 μM) the T_m values for the thermal unfolding process are lower than at the higher concentrations and match those obtained for the apoprotein. This suggests that, at these concentrations, the FMN dissociates in the fluorescence transition and apoprotein stability is probed. At intermediate (5−10 μM) holoprotein concentrations, the T_m values for both fluores-

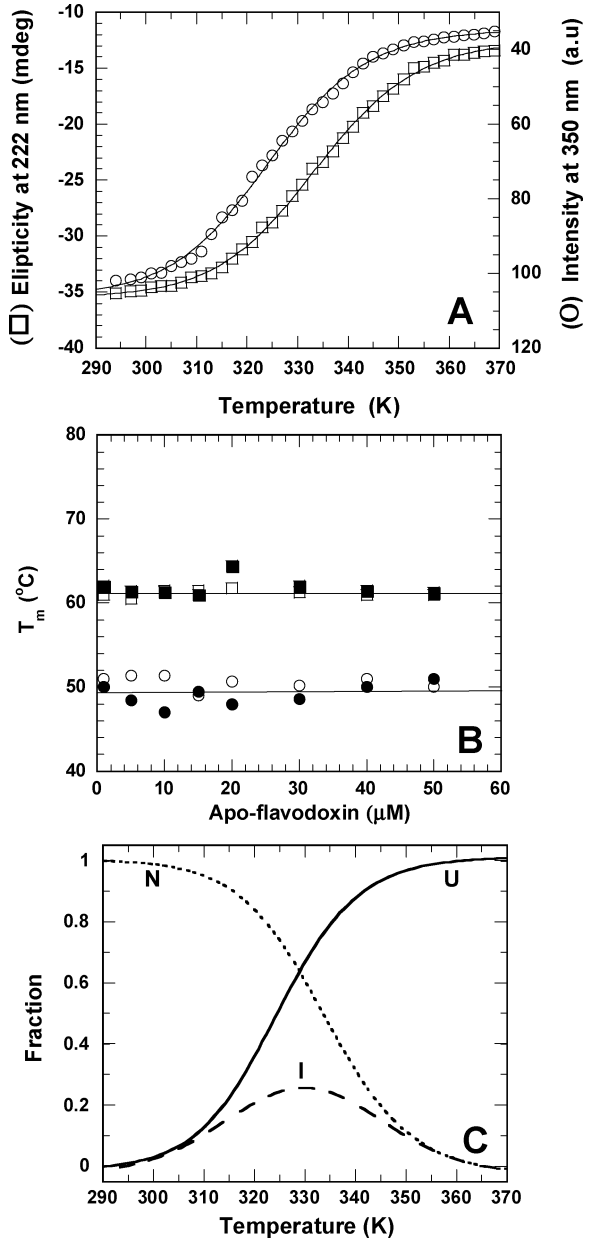

FIGURE 3: Thermal unfolding of apoflavodoxin. (A) Representative unfolding profiles of apoflavodoxin as monitored by fluorescence at 350 nm (circles) and CD at 222 nm (squares) (15 μM protein, 40 mM phosphate, pH 7). Solid lines represent two-state fits used to derive T_m values. (B) T_m values for apoflavodoxin unfolding (open symbols) and refolding (filled symbols) as monitored by fluorescence (circles) and far-UV CD (squares). Lines are drawn to guide the eye. (C) Assuming a three-state mechanism [involving folded (F), intermediate (I), and unfolded (U) species] and that the fluorescence transition reports on the disappearance of the native state and the CD transition reports on formation of the unfolded state, the fraction of intermediate at each temperature was calculated ($1 = f_F + f_I + f_U$).

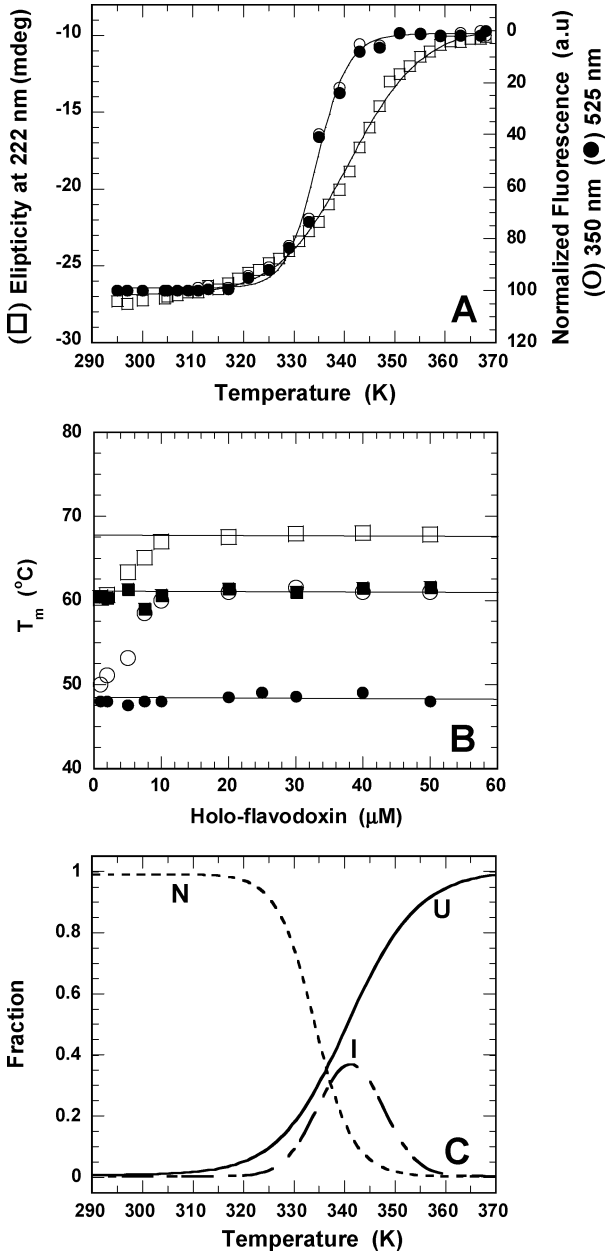

FIGURE 4: Thermal unfolding of holoflavodoxin. (A) Unfolding profiles of holoflavodoxin as monitored by fluorescence at 350 nm (open circles) and at 525 nm (filled circles) and by CD at 222 nm (squares) (10 μM protein, 40 mM phosphate, pH 7). Solid lines represent two-state fits used to derive T_m values. (B) T_m values for holoflavodoxin unfolding (open symbols) and refolding (filled symbols) as monitored by fluorescence (circles) and far-UV CD (squares). Lines are drawn to guide the eye. (C) Assuming a three-state mechanism [involving folded (F), intermediate (I), and unfolded (U) species] and that the fluorescence transition reports on the disappearance of the native state and the CD transition reports on formation of the unfolded state, the fraction of holo intermediate at each temperature was calculated ($1 = f_F + f_I + f_U$).

cence and CD transitions increase as a function of protein concentration to the invariant T_m values found for thermal unfolding of holoflavodoxin at 10 μM and higher protein concentrations. These observations imply that, at high holoprotein concentrations, the FMN remains bound during both thermal transitions. However, FMN's interaction with the unfolded polypeptide may be weak and nonspecific (see below). Assuming again a three-state mechanism involving F, I, and U species, and the constraints that the fluorescence transition reports on the disappearance of the native state and the CD transition reports on formation of the unfolded state, the fraction of holo intermediate at each temperature was calculated (10 μM holoflavodoxin; Figure 4C).

Thermal Refolding of Holoflavodoxin. Thermal unfolding of the holoprotein appears reversible since, upon cooling to 20 °C, the CD and fluorescence signals of the native holoprotein are fully recovered. However, the refolding

Table 1: Thermodynamic Data of the N to I and I to U Equilibria in Apo- and Holoflavodoxin Thermal Unfolding and Spectroscopic Resemblance between the Intermediate and Unfolded States[a]

global fit[b] (protein)	T_{mNI} (K)	$\Delta H(T_m)_{NI}$ (kcal/mol)	T_{mIU} (K)	$\Delta H(T_m)_{IU}$ (kcal/mol)	Z_{Fl}[c]	Z_{CD}[c]	R^2
D. desulfuricans apoflavodoxin	321 ± 1	35 ± 1	336 ± 1	50 ± 2	0.68 ± 0.09	0.16 ± 0.05	0.996
D. desulfuricans holoflavodoxin	328 ± 1	41 ± 2	341 ± 1	56 ± 2	0.46 ± 0.10	0.17 ± 0.02	0.998
Anabaena apoflavodoxin	317	28	330	55	0.7	0.1	

[a] The equilibrium fluorescence- and CD-detected unfolding curves were globally fitted to a three-state model as outlined in Materials and Methods (see also Figure 5). The parameters for *Anabaena* apoflavodoxin (*19*) are shown for comparison. [b] Three to four curves for each technique were included in each global fit. All thermodynamic parameters of the two equilibria were kept identical for all curves while the spectroscopic similarity between the intermediate and the unfolded states (*Z* parameters) was allowed to vary among the two detection techniques. Errors are provided by the fitting program. [c] If $Z = 1$, the intermediate is identical to the unfolded state; if $Z = 0$, the intermediate is identical to the native state.

profiles obtained upon cooling unfolded holoflavodoxin (10 μM and higher protein concentrations) by both detection methods differ from the corresponding unfolding profiles. Upon cooling starting from 95 °C, the far-UV CD and fluorescence profiles give T_m values of 60 and 50 °C (Figure 4B), respectively, which closely resemble the transitions for apoflavodoxin (cf. Figure 3B). This suggests that FMN dissociates from the unfolded holoprotein at the higher temperatures. Rebinding of FMN at such temperatures is thermodynamically unfavorable (low affinity; see below) and appears kinetically inaccessible. We find FMN dissociation from the unfolded holoflavodoxin to be extremely slow. Dialysis experiments of unfolded holoflavodoxin (20 μM protein, 3.5 kDa cutoff membrane) against buffer at 80 °C show that FMN indeed dissociates but that more than 3 h are required to obtain 50% FMN dissociation from the unfolded protein. As a control, the same amount of free FMN leaked out rapidly, within the first 30 min (leakage measured by FMN absorption at 445 nm; data not shown). If FMN dissociation is slow, association will also be slow since the FMN affinity for the unfolded polypeptide is lower than for the folded protein, according to earlier chemical denaturant studies (*21*). Moreover, FMN binding to GuHCl-unfolded apoflavodoxin (20 °C, pH 7) was found to be roughly 1000-fold slower than binding to the folded apoprotein (B. K. Muralidhara and P. Wittung-Stafshede, unpublished results). FMN dissociation at high temperatures combined with negligible rebinding at these conditions explains the cooling data, i.e., that the polypeptide refolds before FMN rebinds. Since all of the holoprotein is recovered in the end of each cooling experiment, FMN does not aggregate at the higher temperatures.

We find the fluorescence and CD transitions for heating and cooling of holoflavodoxin (above 10 μM) to be identical [i.e., T_m values of 60 °C (fluorescence) and 67 °C (CD) for both up and down scans] if the samples are heated to temperatures just below (~80 °C) those resulting in FMN dissociation. This confirms that the two holoflavodoxin transitions are truly reversible, equilibrium transitions, as is also supported by the lack of scan rate and protein concentration dependencies. It is the subsequent FMN dissociation step at higher temperatures that renders pathway reversibility in the cooling experiments which start at 95 °C.

Global Fitting of Thermal Unfolding to the Three-State Model. Albeit used to analyze apoflavodoxin unfolding data in several cases (*18*, *22*), the assumptions made in the three-state analysis shown in Figures 3C and 4C may not be valid. Therefore, we globally fitted the spectroscopic data to a three-state equilibrium unfolding model (F to I to U) using thermal unfolding data for all of the apoprotein concentrations included in Figure 3B and holoflavodoxin concentrations 10 μM and higher (Figure 4B). We followed the approach described by Luo et al. (*28*) in which all of the thermodynamic properties of the two equilibria (native/intermediate and intermediate/unfolded) are globally constrained but the degree of spectroscopic resemblance between the intermediate and the denatured state (the so-called *Z* parameter) is allowed to vary among the techniques used to probe unfolding (see Materials and Methods). In Table 1 we list the obtained parameters [T_{mNI}, T_{mIU}, $\Delta H(T_m)_{NI}$, $\Delta H(T_m)_{IU}$, Z_{Fl}, and Z_{CD}] and R^2 for the three-state global analyses of the thermal behaviors of apoflavodoxin (Figure 5A,B) and holoflavodoxin (Figure 5C,D). The apo and holo intermediates are maximally populated, to about 70%, at 56 and 62 °C, respectively (Figure 5B,D). The apo and holo intermediates appear to be structurally similar: the intermediate has 84% and 83% nativelike CD signal, and 32% and 54% nativelike fluorescence signal, for apo and holo forms, respectively. The global fits show that the assumptions made in Figures 3C and 4C (intermediate has 100% nativelike CD signal and 0% nativelike fluorescence signal) are not correct. The stabilizing effect of the FMN (on the native as well as the intermediate state) is clear when the T_m and $\Delta H(T_m)$ values for both the F/I and I/U transitions are compared (Table 1).

FMN Binding to Apoflavodoxin as a Function of Temperature. FMN binding to apoflavodoxin at different temperatures was tested by isothermal titration calorimetry (ITC) (*31*). FMN fluorescence quenching is not as reliable to probe binding since FMN interactions with unfolded, or partially folded, flavodoxin do not affect the FMN emission to a large extent (*21*, *22*). FMN-binding experiments to apoflavodoxin (40 mM phosphate, pH 7) were performed at 20, 40, 50, 60, 65, and 70 °C (Figure 6). The binding data at 20, 40, and 50 °C were fit to a single set of binding sites with the resulting parameters: stoichiometry *n* of 1.0 ± 0.1 (all three temperatures) and K_D of ~0.1 μM (20 and 40 °C) and ~1.0 μM (50 °C). At 50 °C, the apoprotein sample consists of ~40% native and 60% intermediate species (Figure 5B). Since stoichiometric FMN binding is detected, it suggests that also the intermediate species can bind FMN. The created holoprotein at 50 °C should, at equilibrium, consist of a mixture of ~70% native and 30% intermediate species (Figure 5D); thus half of the apo intermediates should fold upon FMN binding. The estimated K_D at 50 °C is thus an average of FMN affinities for folded and intermediate apo forms and also includes effects of folding.

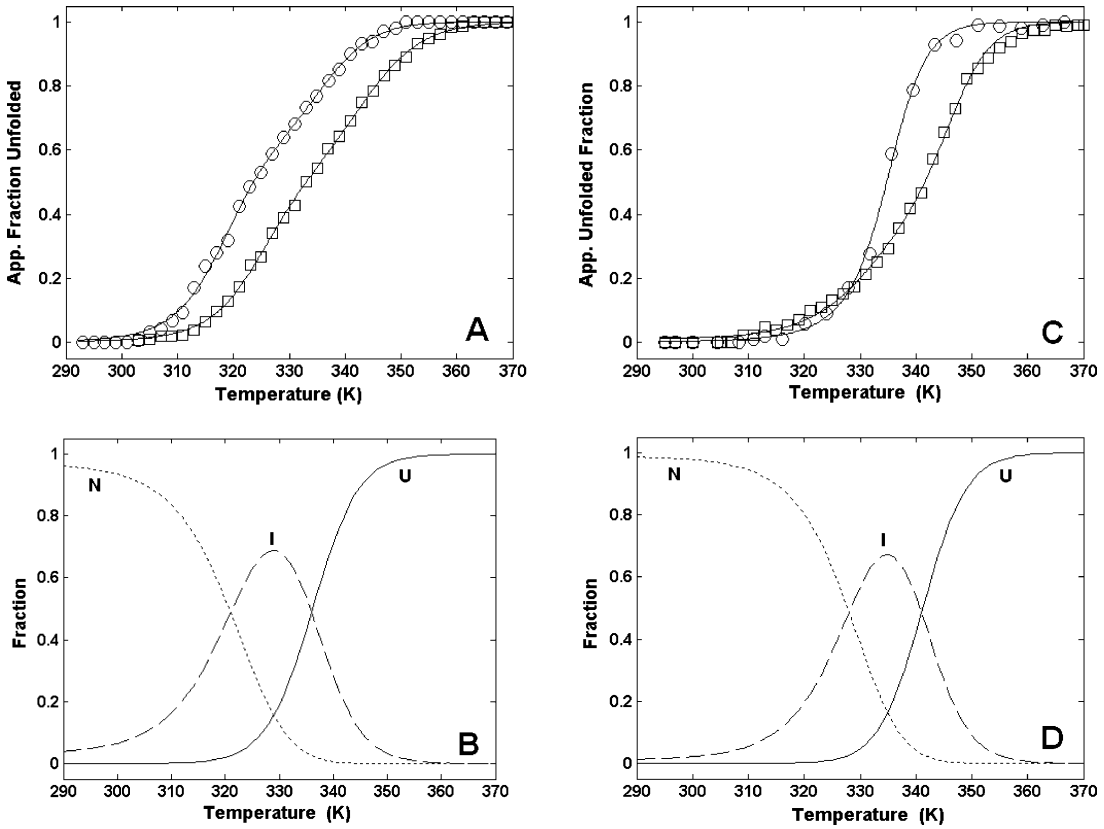

FIGURE 5: Global fitting of thermal data to a three-state model. (A) Curves corresponding to the global fit (Table 1) are shown on top of experimental CD and fluorescence data for apoflavodoxin. (B) Fraction of folded, unfolded, and intermediate species as a function of temperature corresponding to the global fit for apoflavodoxin unfolding is shown. (C) Curves corresponding to the global fit (Table 1) are shown on top of experimental CD and fluorescence data for holoflavodoxin. Since the transitions obtained by fluorescence at 350 and 525 nm overlap, these data points were combined for data analysis. (D) Fraction of folded, holo unfolded, and holo intermediate species as a function of temperature corresponding to the global fit for holoflavodoxin unfolding is shown.

Significant FMN binding was also observed at 60°C where the apo sample consists of roughly 5% folded, 60% apo intermediate, and 35% unfolded species according to Figure 5B. At this temperature, the holoprotein population consists of over 65% intermediate species (Figure 5D). Since FMN binding, which appears to saturate, is observed at this temperature, it supports that the apo intermediate can bind FMN and, thus, that the holo intermediate species can exist. This is in agreement with the thermal unfolding experiments, which indicate that the FMN remains bound to holoflavodoxin until polypeptide unfolding is completed. At 65 °C (where the apoprotein sample is dominated by unfolded species) weak binding was observed; at 70 °C no FMN binding at all was observed (even for 100 μM protein titrated with 2 mM FMN; not shown). Due to the complexity of the reactions, attempts to analyze the binding data above 50 °C failed. Nonetheless, the FMN-binding experiments qualitatively show, as expected, that the FMN affinity for apoflavodoxin decreases as the temperature is increased, which supports that FMN dissociation will occur at high temperatures. The ITC data are also in agreement with the observation that FMN does not rebind promptly to the apoprotein until temperatures around 50 °C are reached in the cooling experiments starting from 95 °C.

DISCUSSION

Does a protein's structure dictate the folding pathway, so that proteins within the same structural family would fold in similar ways? The flavodoxin-like fold is a common structural motif found in many protein superfamilies with very different functions (*12*). In the case of flavodoxin, the active site consists of a flavin cofactor (FMN) that coordinates to residues in three loops of the protein (*13*, *15*). In vitro unfolding experiments on the apo forms of several long-chain flavodoxins have shown that thermal unfolding proceeds through a rather stable, nativelike intermediate (*17*−*19*). To address, for the first time, the thermal unfolding pathway for a short-chain flavodoxin and also the role of the FMN cofactor in this process, we here compare the thermal unfolding reactions for apo and holo forms of the short-chain *D. desulfuricans* flavodoxin (Figure 1). Although cofactors, such as FMN, often stabilize the native states of proteins (*32*−*35*), the manner in which cofactors affect polypeptide folding processes is not well understood.

We find that, upon heating, *D. desulfuricans* apoflavodoxin unfolds in a three-state equilibrium process (F to I to U): first there is a fluorescence-detected transition and then there is a far-UV CD transition (Figure 3). Thus, an intermediate structure is populated during the reaction that is, according to global analysis, 65% similar to the unfolded state in terms of fluorescence but 90% similar to the folded state in terms of secondary structure (Table 1). The thermal unfolding behavior for *D. desulfuricans* apoflavodoxin mimics the behavior of the long-chain *A. vinelandii* and *Anabaena* PCC 7119 apoflavodoxins (*18*, *19*). Thermal midpoints occur at 43.5, 48, and 50 °C, when probed by fluorescence, and at 57, 62, and 60 °C, when probed by far-UV CD, for *Anabaena* PCC 7119 (pH 7, 50 mM Mops), *A. vinelandii* (pH 6, 100

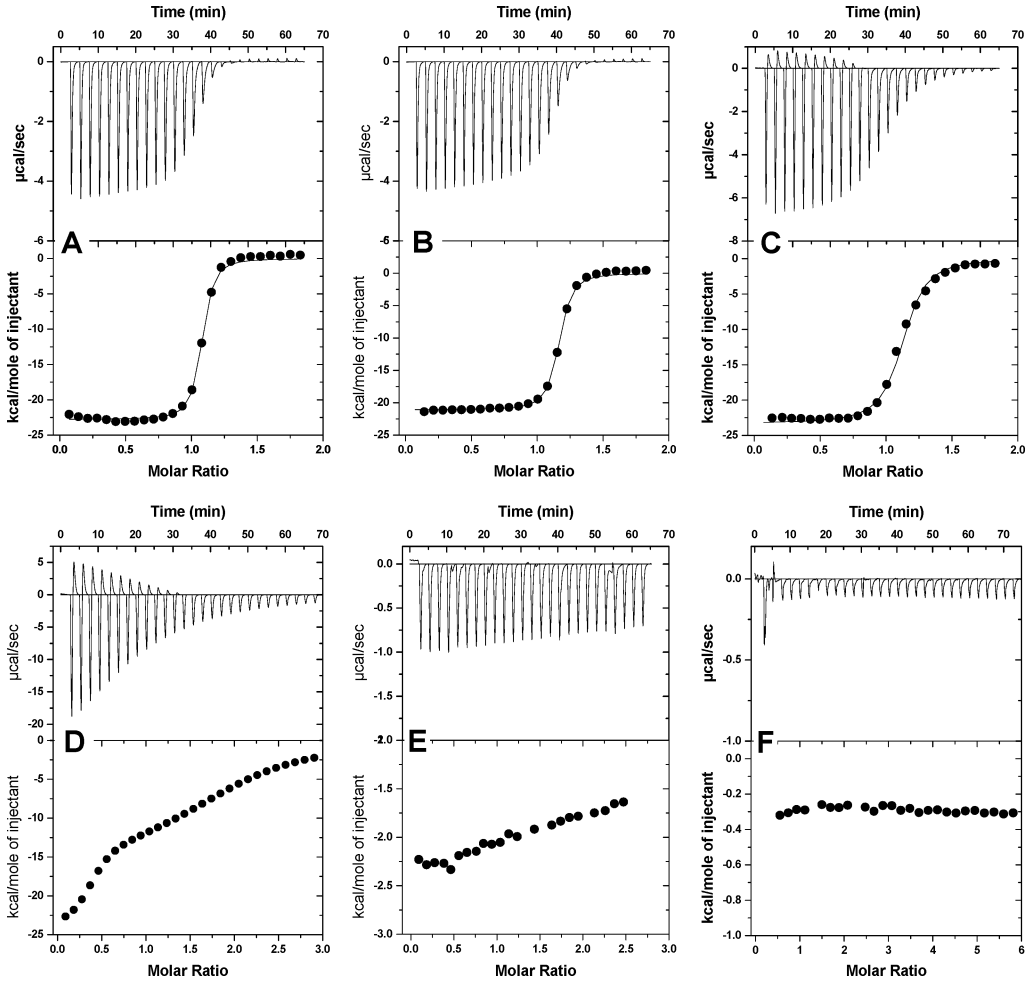

FIGURE 6: Cofactor binding to apoflavodoxin at various temperatures. FMN binding to apoflavodoxin studied by ITC at (A) 20 °C, (B) 40 °C, (C) 50 °C, (D) 60 °C, (E) 65 °C, and (F) 70 °C. The upper panels show the heat changes upon FMN additions to 50 μM apoflavodoxin in the cell; the lower panels show the resulting binding isotherms for 20, 40, and 50 °C. The data at higher temperatures were not fitted.

mM phosphate), and *D. desulfuricans* (pH 7, 40 mM phosphate) apoflavodoxins, respectively. The structure of the apo intermediate from *Anabaena* PCC 7119 was probed by mutagenesis, and it was concluded that the intermediate's topology and surface tertiary interactions are close to nativelike (*19*). This indicates that hydrogen bonding on the surface contributes to the conformation and energetics of the *Anabaena* apoflavodoxin intermediate (*19*). The global fitting parameters for the three-state model [T_{mNI}, T_{mIU}, $\Delta H(T_m)_{NI}$, $\Delta H(T_m)_{IU}$, Z_{Fl}, and Z_{CD}; Table 1] are very similar for *D. desulfuricans* and for *Anabaena* apoflavodoxin, suggesting that these two species adopt closely related, with respect to both structure and stability, thermally induced equilibrium intermediates.

Like the apoprotein, thermal unfolding (pH 7, 40 mM phosphate) of *D. desulfuricans* holoflavodoxin also involves a populated intermediate (Figure 4). First there is a transition monitored by fluorescence and then there is a far-UV CD-detected transition. At holoprotein concentrations 10 μM and higher, both thermal transitions are stabilized by the presence of the cofactor: the individual T_m values are increased by ~10 °C as compared to the apoflavodoxin transitions. Since the fluorescence- and CD-detected T_m values are higher for the holoprotein (at 10 μM and higher concentrations), the transitions are fully reversible as long as heating does not go above ~80 °C, and they exhibit no protein concentration dependence, FMN remains bound to the polypeptide during both steps. This is reasonable since FMN was earlier shown to remain bound to *D. desulfuricans* flavodoxin upon GuHCl-induced unfolding (*21*, *22*). Upon comparison of the global fitting data for the holo (10 μM and higher protein concentrations) and apo forms of flavodoxin (Table 1, Figure 5), it emerges that the holo intermediate, like the apo intermediate, has nativelike secondary structure but a more unfolded-like fluorescence signal. The apo intermediate appears to have more unfolded-like fluorescence characteristics than the holo intermediate; however, the origins of the fluorescence signals are different (tryptophan emission in the case of the apoprotein; FMN quenching due to tryptophan stacking in the case of the holoprotein). Formation of both apo and holo intermediates involves weakening, by roughly 40%, of the interactions that contribute to the enthalpic stabilization of the native states. Both intermediates thus still display substantial enthalpic stability relative to the unfolded states. The presence of the cofactor affects the stability of the native and intermediate states in similar manners. The T_m for the folded to intermediate transition increases by 7 °C, and that for the intermediate to unfolded transition increases by 6 °C, when the FMN is present. The overall enthalpic stabilization of folded flavodoxin, relative to the

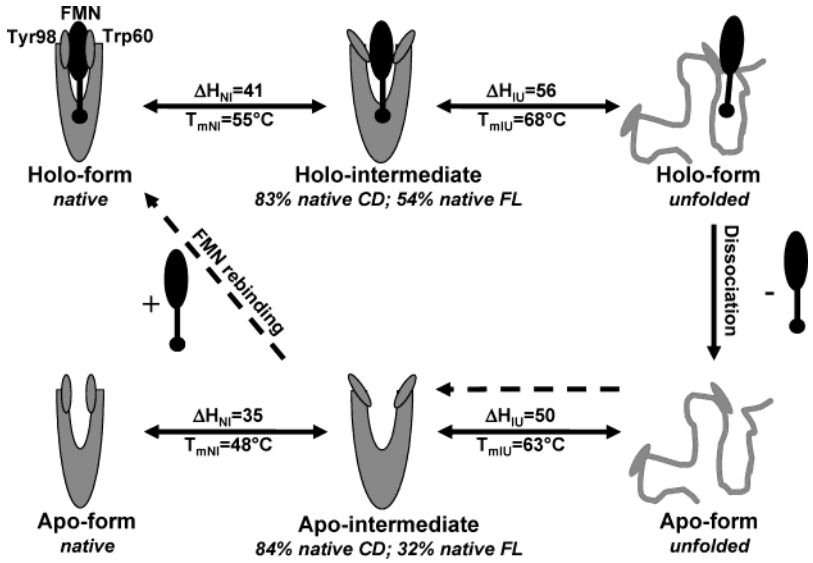

FIGURE 7: Pathways for thermal unfolding of *D. desulfuricans* apo- and holoflavodoxin. Apoflavodoxin unfolds via an intermediate (84% nativelike with respect to secondary structure) that subsequently converts to the unfolded state in a reversible process (bottom row in scheme). Holoflavodoxin (10 μM and higher) also unfolds via an intermediate (83% nativelike with respect to secondary structure), which is stabilized by the presence of the bound cofactor as compared to the apo intermediate. The holo intermediate then converts to the unfolded state (upper row in scheme), which is subsequently (if heating is continued) followed by FMN dissociation. Since FMN association at high temperatures is kinetically inaccessible, refolding upon cooling of the holoprotein follows the pathway of the apoprotein. FMN rebinding occurs during conversion of the apo intermediate to the native protein (i.e., at temperatures below 50 °C) (dashed arrows indicate the refolding pathway for the holoprotein). Double-sided arrows represent reversible processes. FMN and the two aromatic residues (Trp60 and Tyr98) are labeled; the thermal midpoint and $\Delta H(T_m)$ (in kcal/mol) for each step as deduced from the global fits are indicated.

unfolded form, is increased by 15% by the FMN interactions (Table 1). In Figure 7, we have summarized the observed thermal unfolding pathways, and the corresponding thermodynamic parameters, for apo and holo forms of *D. desulfuricans* flavodoxin.

To date, thermal unfolding has been characterized for three species of apoflavodoxin: *A. vinelandii* (*18*), *Anabaena* (*19*), and *D. desulfuricans* (this work). In all cases does the reaction involve a nativelike intermediate. Thus, a thermal three-state equilibrium unfolding pathway appears to be conserved among long- and short-chain as well as apo and holo forms of flavodoxins. Also, another protein with the flavodoxin-like fold, *E. coli* CheY, was shown to unfold via a thermal intermediate (*36*), suggesting that it may be a general pathway for thermal unfolding of proteins with this folding motif. Moreover, the thermal intermediate may be structurally related to kinetic intermediates formed during *Anabaena* and *D. desulfuricans* apoflavodoxin refolding reactions (*21*, *37*). In contrast to the invariant thermal behavior, chemically induced equilibrium unfolding varies between two and three state among the above-mentioned flavodoxins (*18*, *21*, *22*). *D. desulfuricans* is the only holoflavodoxin that has been studied with respect to chemically and thermally induced equilibrium unfolding: the cofactor does not affect the unfolding pathway, although it is found to stabilize the protein toward both chemical (*21*) and thermal perturbation.

ACKNOWLEDGMENT

We thank Prasad Dharap (Civil and Environmental Engineering), Sushant M. Dutta (Mechanical Engineering and Material Science), and Corey J. Wilson (Biochemistry and Cell Biology) of Rice University for help with the global fitting.

REFERENCES

1. Jackson, S. E. (1998) How do small single-domain proteins fold?, *Folding Des. 3*, R81−R91.
2. Privalov, P. L. (1996) Intermediate states in protein folding, *J. Mol. Biol. 258*, 707−725.
3. States, D. J., Creighton, T. E., Dobson, C. M., and Karplus, M. (1987) Conformations of intermediates in the folding of the pancreatic trypsin inhibitor, *J. Mol. Biol. 195*, 731−739.
4. Fersht, A. (1999) *Structure and Mechanism in Protein Science*, W. H. Freeman, New York.
5. Wittung-Stafshede, P. (2002) Role of cofactors in protein folding, *Acc. Chem. Res. 35*, 201−208.
6. Wittung-Stafshede, P., Lee, J. C., Winkler, J. R., and Gray, H. B. (1999) Cytochrome *b*562-folding triggered by electron transfer: approaching the speed limit for formation of a four-helix-bundle protein, *Proc. Natl. Acad. Sci. U.S.A. 96*, 6587−6590.
7. Wittung-Stafshede, P., Malmstrom, B. G., Winkler, J. R., and Gray, H. B. (1998) Electron-transfer triggered folding of deoxymyoglobin, *J. Phys. Chem. 102*, 5599−5601.
8. Wittung-Stafshede, P., Malmstrom, B. G., Sanders, D., Fee, J. A., Winkler, J. R., and Gray, H. B. (1998) Effect of redox state on the folding free energy of a thermostable electron-transfer metalloprotein: the CuA domain of cytochrome oxidase from *Thermus thermophilus*, *Biochemistry 37*, 3172−3177.
9. Leckner, J., Wittung, P., Bonander, N., Karlsson, G., and Malmstrom, B. (1997) The effect of redox state on the folding free energy of azurin, *J. Biol. Inorg. Chem. 2*, 368−371.
10. Pozdnyakova, I., and Wittung-Stafshede, P. (2001) Copper binding before polypeptide folding speeds up formation of active (holo) *Pseudomonas aeruginosa* azurin, *Biochemistry 40*, 13728−13733.
11. Pozdnyakova, I., and Wittung-Stafshede, P. (2001) Biological relevance of metal binding before protein folding, *J. Am. Chem. Soc. 123*, 10135−10136.
12. Muller, F. (1992) *Chemistry and Biochemistry of Flavoenzymes*, CRC Press, Boca Raton, FL.
13. Watenpaugh, K. D., Sieker, L. C., and Jensen, L. H. (1973) The binding of riboflavin-5′-phosphate in a flavoprotein: flavodoxin at 2.0-angstrom resolution, *Proc. Natl. Acad. Sci. U.S.A. 70*, 3857−3860.
14. Lostao, A., El Harrous, M., Daoudi, F., Romero, A., Parody-Morreale, A., and Sancho, J. (2000) Dissecting the energetics of the apoflavodoxin-FMN complex, *J. Biol. Chem. 275*, 9518−9526.

15. Genzor, C. G., Perales-Alcon, A., Sancho, J., and Romero, A. (1996) Closure of a tyrosine/tryptophan aromatic gate leads to a compact fold in apo flavodoxin, *Nat. Struct. Biol. 3*, 329−332.
16. Steensma, E., and van Mierlo, C. P. (1998) Structural characterisation of apoflavodoxin shows that the location of the stable nucleus differs among proteins with a flavodoxin-like topology, *J. Mol. Biol. 282*, 653−666.
17. van Mierlo, C. P., and Steensma, E. (2000) Protein folding and stability investigated by fluorescence, circular dichroism (CD), and nuclear magnetic resonance (NMR) spectroscopy: the flavodoxin story, *J. Biotechnol. 79*, 281−298.
18. van Mierlo, C. P., van Dongen, W. M., Vergeldt, F., van Berkel, W. J., and Steensma, E. (1998) The equilibrium unfolding of *Azotobacter vinelandii* apoflavodoxin II occurs via a relatively stable folding intermediate, *Protein Sci. 7*, 2331−2344.
19. Irun, M. P., Garcia-Mira, M. M., Sanchez-Ruiz, J. M., and Sancho, J. (2001) Native hydrogen bonds in a molten globule: the apoflavodoxin thermal intermediate, *J. Mol. Biol. 306*, 877−888.
20. Genzor, C. G., Beldarrain, A., Gomez-Moreno, C., Lopez-Lacomba, J. L., Cortijo, M., and Sancho, J. (1996) Conformational stability of apoflavodoxin, *Protein Sci. 5*, 1376−1388.
21. Apiyo, D., and Wittung-Stafshede, P. (2002) Presence of the cofactor speeds up folding of *Desulfovibrio desulfuricans* flavodoxin, *Protein Sci. 11*, 1129−1135.
22. Apiyo, D., Guidry, J., and Wittung-Stafshede, P. (2000) No cofactor effect on equilibrium unfolding of *Desulfovibrio desulfuricans* flavodoxin, *Biochim. Biophys. Acta 1479*, 214−224.
23. Nuallain, B. O., and Mayhew, S. G. (2002) A comparison of the urea-induced unfolding of apoflavodoxin and flavodoxin from *Desulfovibrio vulgaris*, *Eur. J. Biochem. 269*, 212−223.
24. Helms, L. R., and Swenson, R. P. (1991) Cloning and characterization of the flavodoxin gene from *Desulfovibrio desulfuricans*, *Biochim. Biophys. Acta 1089*, 417−419.
25. Caldeira, J., Palma, P. N., Regalla, M., Lampreia, J., Calvete, J., Schafer, W., Legall, J., Moura, I., and Moura, J. J. (1994) Primary sequence, oxidation−reduction potentials and tertiary-structure prediction of *Desulfovibrio desulfuricans* ATCC 27774 flavodoxin, *Eur. J. Biochem. 220*, 987−995.
26. Romero, A., Caldeira, J., Legall, J., Moura, I., Moura, J. J., and Romao, M. J. (1996) Crystal structure of flavodoxin from *Desulfovibrio desulfuricans* ATCC 27774 in two oxidation states, *Eur. J. Biochem. 239*, 190−196.
27. Muralidhara, B. K., and Wittung-Stafshede, P. (2003) Can cofactor-binding sites in proteins be flexible? *Desulfovibrio desulfuricans* flavodoxin binds FMN dimer, *Biochemistry 42*, 13074−13080.
28. Luo, J., Iwakura, M., and Matthews, C. R. (1995) Detection of a stable intermediate in the thermal unfolding of a cysteine-free form of dihydrofolate reductase from *Escherichia coli*, *Biochemistry 34*, 10669−10675.
29. Privalov, P. (1997) Thermodynamics of protein folding, *J. Chem. Thermodyn. 29*, 447−474.
30. Privalov, P. L., and Potekhin, S. A. (1986) Scanning microcalorimetry in studying temperature-induced changes in proteins, *Methods Enzymol. 131*, 4−51.
31. Lopez, M. M., and Makhatadze, G. I. (2002) Isothermal titration calorimetry, *Methods Mol. Biol. 173*, 121−126.
32. Robinson, C. R., Liu, Y., Thomson, J. A., Sturtevant, J. M., and Sligar, S. G. (1997) Energetics of heme binding to native and denatured states of cytochrome *b*562, *Biochemistry 36*, 16141−16146.
33. Bertini, I., Cowan, J. A., Luchinat, C., Natarajan, K., and Piccioli, M. (1997) Characterization of a partially unfolded high potential iron protein, *Biochemistry 36*, 9332−9339.
34. Leckner, J., Bonander, N., Wittung-Stafshede, P., Malmstrom, B. G., and Karlsson, B. G. (1997) The effect of the metal ion on the folding energetics of azurin: a comparison of the native, zinc and apoprotein, *Biochim. Biophys. Acta 1342*, 19−27.
35. Goedken, E. R., Keck, J. L., Berger, J. M., and Marqusee, S. (2000) Divalent metal cofactor binding in the kinetic folding trajectory of *Escherichia coli* ribonuclease HI, *Protein Sci. 9*, 1914−1921.
36. Filimonov, V. V., Prieto, J., Martinez, J. C., Bruix, M., Mateo, P. L., and Serrano, L. (1993) Thermodynamic analysis of the chemotactic protein from *Escherichia coli*, CheY, *Biochemistry 32*, 12906−12921.
37. Fernandez-Recio, J., Genzor, C. G., and Sancho, J. (2001) Apoflavodoxin folding mechanism: an alpha/beta protein with an essentially off-pathway intermediate, *Biochemistry 40*, 15234−15245.

BI048944E